8/26/94

Solar Wind Features Responsible for Magnetic Storms and Substorms during the Declining Phase of the Solar Cycle: 1974

B. "J'. Tsurutani and J. K. Arballo
Space Physics and Astrophysics Section,
Jet Propulsion Laboratory, California Institute of Technology, Pasadena, California, 91109

W. D. Gonzalez and A. I.. C. Gonzalez
Instituto Nacional Pesquisas Espaciais, Sao Jose dos Campos, San Paulo, Brazil

F. Tang
California Institute of Technology, Pasadena, California, 91125

M. Okada
National Institute of Polar Research, Tokyo, Japan

ABSTRACT

We examine interplanetary data and geomagnetic activity indices (D_{ST}, AE, Kp) during 1974 when two long-lasting solar wind corotating streams existed. We find that only 3 major storms ($D_{ST} \leq$ -100 nT) occurred during 1974, and all were associated with coronal mass ejections (CMEs). Each high speed stream was led by a shock, so the three storms had sudden commencements. Two of the 1974 major storms were associated with shock compression of preexisting southward fields and one was caused by southward fields within a magnetic cloud. Corotating streams were responsible for recurring moderate (-100 nT $\leq D_{ST} \leq$ -50 nT) to weak (.50 nT $\leq D_{ST} \leq$ -25 nT) magnetic storms. However, some corotating streams had little or no ring current effects at all ($D_{ST} \geq$ -25 nT). Because these streams have higher velocities than the typical solar wind at 1 AU, they often arc preceded in time by the passage of the heliospheric current sheet (HCS) crossings and their high density plasma sheets(~50 cm-3). The enhanced ram pressure associated with the plasma sheet passage causes a "storm initial phase". This phase dots not have a "sudden commencement" due to the lack of a shock. Thus, the physical cause for these storm initial phases is quite different from storms associated with fast CMEs. The causes of moderate and weak magnetic storms arc associated with intense magnetic fields (1 5-25 nT) generated at the corotating stream/HCS interaction regions. When the fields have southward components, geomagnetic activity results. However, it appears that the stream/I ICS interaction crcatcs southward components that last only short durations of time (< 3 hours), so that major magnetic storms generally do not result.

The most dramatic magnetospheric effect of corotating streams is continual auroral activity called High Intensity Long Duration Continuous AE Activity (HILDCAA). HILDCAAs are caused by magnetic reconnection through the southward component of interplanetary Alfvén waves. The Alfvén waves begin with the corotating stream onset and gradually fade away as the velocity of the stream and the Alfvén wave amplitudes decrease. In 1974, these 27-day recurring events lasted 10 days or longer. It is the HILDCAAs associated with the two corotating streams pcr solar rotation that lead to the exceptionally high AE annual average (283 nT), a value that was substantially higher than that during solar maximum [AE (1979) = 221 nT]. The question "do coronal holes cause 27 day recurring geomagnetic storms" can now bc answered: yes, but only moderate or weak ones. This not only verifies the Chapman and Bartels (1940) result, but now gives the physical reason why 27-day recurrent storms are less intense.

Solar features associated with the CME releases were extremely difficult to find. We do not know if this is typical for this phase of the solar cycle or not. The CMEs were often located near a HCS crossing.

The substorms within HILDCAAs typically have a one-to-one relation with D_{ST} decreases, indicating that these substorms are responsible for substantial particle injection into the middle magnetosphere. This is relevant to the present Workshop. Because of this continuous sporadic (substorm) injection, storms associated with corotating streams often have "recovery" phases that are poorly defined.

In 1940, Chapman and Bartels discussed storms which recur at 27 day intervals. Because there were no visible features on the sun that were correlated with such storms (such as flares), they ascribed the solar source as being due to activity at M (for magnetically effective) regions (Bartels, 1938). On the other hand, CMEs are impulsive events (Hundhausen, 1993) which are believed to occur at times when the instability criteria at helmet streamers are met (Wolfson et al., 1987; Low and Smith, 1993). *One* would therefore not expect this mechanism to cause storms at Earth with any regularity. Clearly, there must be another solar source for recurrent geomagnetic activity.

We now know that these M-regions must be coronal holes. During "and near solar minimum, polar coronal holes can extend down to the equator and can remain there for months or longer (Zirker, 1977). The high speed solar wind coming from these holes is continuously emitted, and because the hole is (relatively) fixed at the Sun, the high speed stream "corotates" with the Sun's rotational period. Thus, if the hole extends to the ecliptic plane, the corotating stream engulfs the Earth's magnetosphere once every 27 days.

In this paper we explore the interplanetary causes of geomagnetic activity during 1974 and examine the geoeffectiveness of high speed corotating streams emanating from coronal holes. Clearly, features of corotating streams leading to geomagnetic activity may be substantially different from those for CMEs. As one example, one would not expect the presence of intense magnetic clouds with large north-south orientations (Klein and Burlaga, 1982, Farrugia et al. 1993a, b) to be present in the corotating streams. Also, because the plasma is continuously (not impulsively) emitted from coronal holes, fast forward shocks can only form at the corotational interface where the stream-stream interaction is a glancing one. Typically shocks at the corotating stream interface are not thought to form until distances greater than -1.5 AU from the Sun (Smith and Wolfe, 1976).

RESULTS

I. Large Scale Structures

High Speed Stream and Magnetic Field Structures

Figures 1 and 2 "illustrate hourly averages of the magnetic field and plasma data and geomagnetic indices for the year 1974. In Figure 1, from top to bottom, arc the interplanetary magnetic field B_Z component in GSM coordinates, D_{ST}, solar wind velocity and the magnetic field magnitude. Figure 2, to the same scale, has B_x, By, solar wind ion density and temperature. At the top of both Figures, the IMF sector crossings are indicated by vertical marks, with the+ and - signs indicating positive and negative sectors. The sector crossings were taken from Svalgaard (1976). These values were derived from the Stanford solar magnetographs.

Examining the overall solar wind velocity features, one can clearly note that there arc predominantly two main streams that occur during each solar rotation of ~ 27 days. This is most obvious for the consecutive 27-day periods of days 24, 51,78, 105, 132, 159, 186,213 and 240. Stream onsets arc present at each of those days. This sequence also extends back in time into 1973 and also forward into 1975, but with less apparent regularity as the events

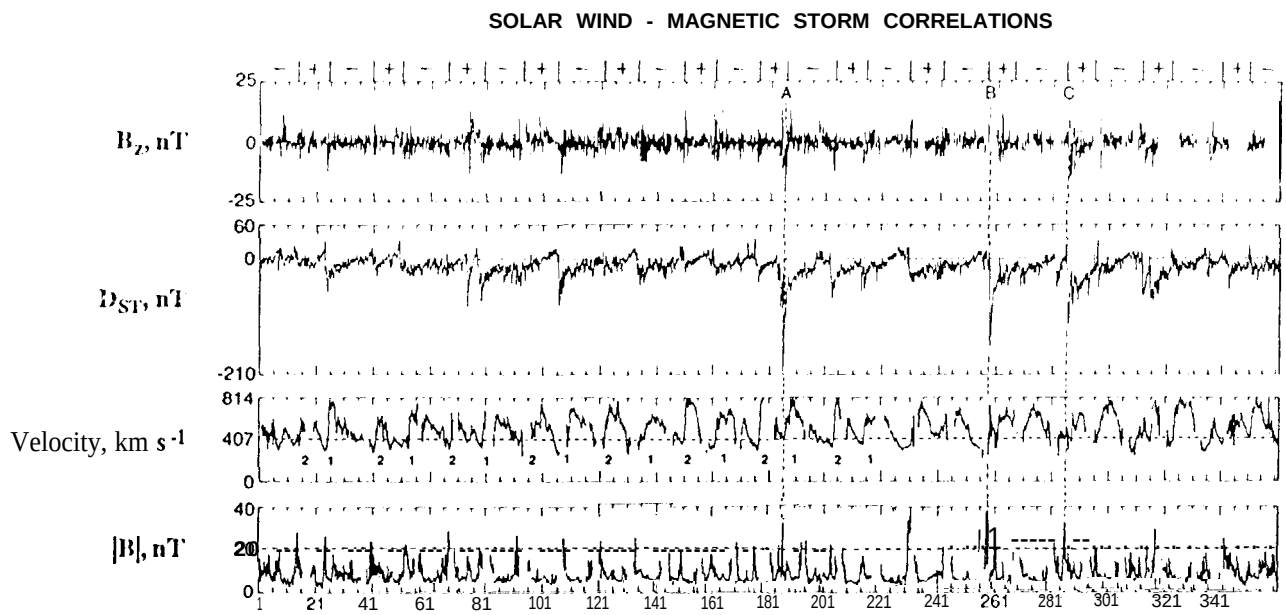

Figure 1. **The IMF B_Z, DST, V_{SW}** and **IMF** |B| for 1974. **The** three largest intensity magnetic stares are **called** out **as the A,** B and C **events. These** storms are caused by impulsive solar events **(CMEs)** and **are** not related **to corotating** streams. **The sectors** arc **denoted** at the **top** of **the** figure.

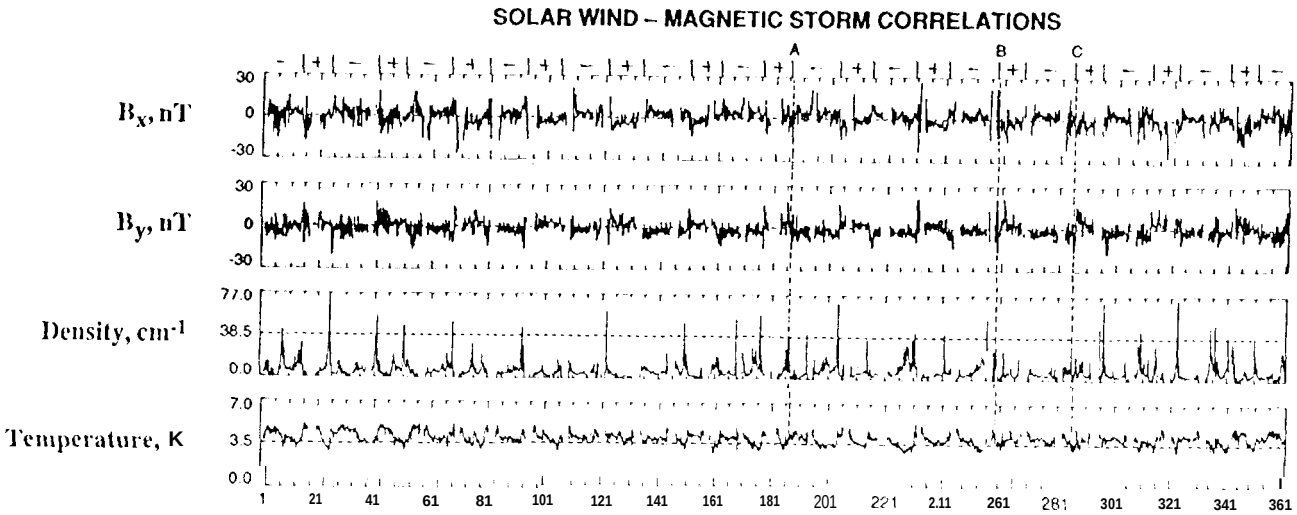

Figure 2. Same format as Figure 1, but for IMF FIX, B_y, N and T.

discussed above. For organizational purposes, wc will refer to this recurring stream as the sequence 1 stream. A second sequence of streams, located in between the sequence 1 streams arc found on days: 15,41, 68,95, 122, 150, 177, 204, and 231. We will refer to this second set as sequence 2 streams. Beyond day 231, the streams become somewhat more complex, so wc will focus on the first 2/3 of the year.

The bottom panel of Figure 1 is the magnetic field magnitude. '1'here arc several features that onc should note. First, the field strength is, in general, anticorrelated with the solar wind velocity, The magnetic field intensity is lowest (below average) when the spacecraft is within a high speed stream, particularly at and near the peak velocity and within the trailing portion of the stream. The highest field magnitudes that occurred during the year appear as spikes on these time scales. Most of these arc located at the leading edges of the high velocity streams. Almost all of tbc large fields that have hourly averages greater than 15 nT arc of this type. Examples arc present on days 25-26, 150-151, 161-162, 176-177, 187, and 204. None of these events arc associated with interplanetary shocks. The maximum peak (hourly average) intensities for these events mentioned above lic in the range of 15 to 25 nT.

Interplanetary Events Causing Magnetic Storms (D_{ST})

The second panel of Figure 1 is the hourly average D_{ST} values for the year. There arc two notable features in this data set. The first is there arc only a few large magnetic storms during the entire year, only three storms with D_{ST} intensities less than -100 nT. These arc event A, on day 187 (D_{ST} = -205 nT), event B on day 257 (D_{ST} = -140 nT), and event C (D_{ST} = -115 nT) on day 285. None of these three events is associated with the two corotating stream sequences discussed previously. All three of the high speed stream events arc led by fast forward shocks.

The storm intensities associated with the sequence 1 and 2 stream structures arc only modest at best. As noted above, from day 1 to day 241, during 9 solar rotations and 18 major corotating stream appearances, there arc only 3 stream appearances associated with $D_{ST} \leq -70$ n"]' values. Most (12 out of 18 events) of the above high speed streams cause only small D_{ST} disturbances of $D_{ST} \geq -50$ nT. Sometimes the geomagnetic disturbances were not even perceptible in the D_{ST} index. Examples of this latter type of stream-storm relationship (small, ≥ -25 nT disturbances , or no storm at all) arc present on days: 15,41,68, 95, 123, 134, 150, 162, 177, 231 and 241. The peak velocity, velocity gradient and peak magnetic fields of these streams arc not much different from those that cause storms with greater intensity $D_{ST} \leq -70$ nT. Other parameters arc important additional factors.

Geoeffectiveness of the Two Corotating Stream Sequences

The two stream sequences, vary in their geoeffectiveness from solar rotation to rotation, and over their stream lifetimes. Of the two sequences, the first is slightly more geoeffective at the beginning of the interval studied, Sequence 1, starting on day 25, and progressing at 27 day intervals, caused peak D_{ST} values of: -65,-20,-75,-85,-45, -30, "A", -60 and -35 nT. The seventh event of the sequence near event A is indeterminate because the large "A" storm overshadows any activity associated with the corotating stream. From Figure 1, the reader can note that the velocity of the stream decreases steadily throughout the event. The peak velocity starts near - 800 km s^{-1} and declines to - 600 km s^{-1} near the end of the sequence. The geoeffectiveness (D_{ST} intensity) of the stream is not directly related to the stream velocity, however. All onc can say is that D_{ST} appears to be slightly more negative at the beginning of the sequence when the velocity was the highest.

D_{ST} Recovery

Another feature to note in the D_{ST} panel of Figure 1 is the very long recovery phases for the moderate and weak magnetic storms generated by the corotating high speed streams. Most recoveries last one week or even longer, or until the next stream arrives. This is substantially different than for storms that occur at and near solar maximum (a standard decay time of the solar maximum storms is < 10 hours, Gonzalez et al. , 1989). In this Figure, long recovery phases arc the rule rather than the exception. Examples of this arc found on days 25 to 35, 80 to 92, 108 to 122 for the sequence 1 streams and days 204 to 214 and 231 to 241 for the sequence 2 streams.

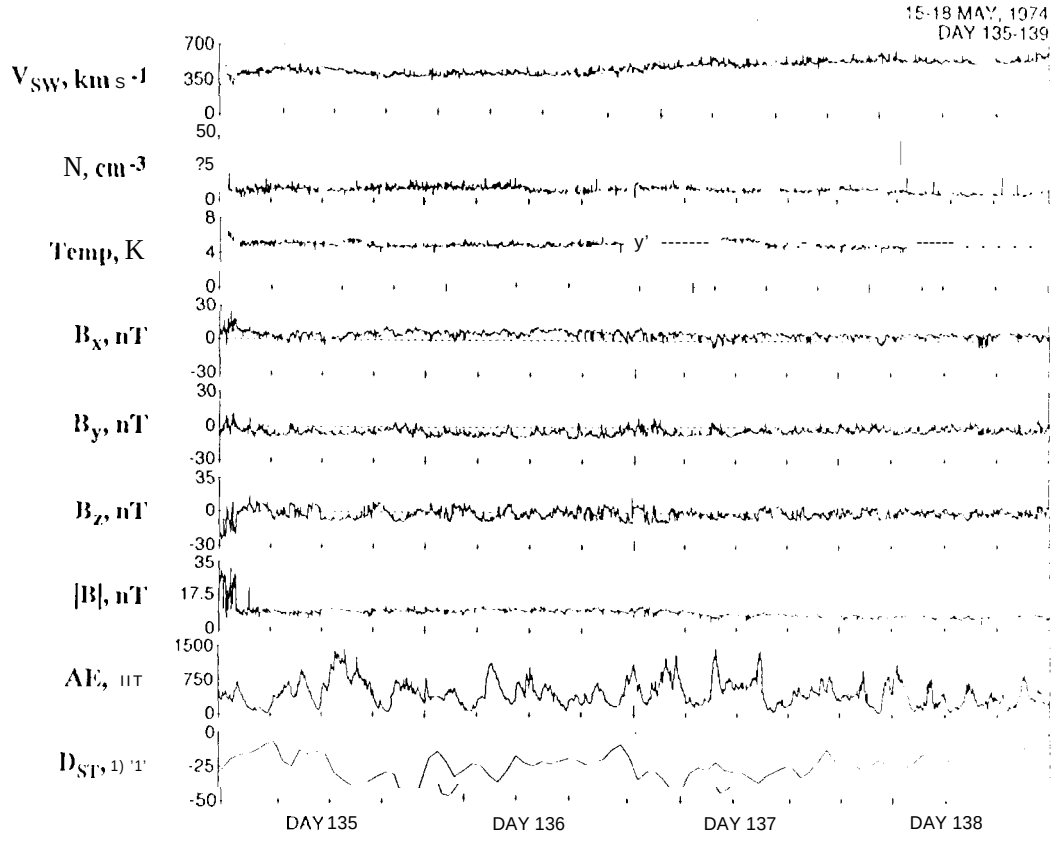

Figure 3. D_{ST} in a "recovery" phase of a magnetic storm. V_{SW}, N, '1', the IMF, AE and 1 D_{ST} for days 135 to 138, 1974. The ring current does not have a classic decay profile, but is within the range of ~- 10 to -50 nT for days. D_{ST} decreases arc associated with southward IMF B_Z events and AE increases. Presumably, magnetic reconnection through the B_Z southward turnings cause the injections of fresh plasma into the magnetosphere, leading to slight increases in the ring current intensity.

There arc other, long-lasting, 10 W-ICVCI D_{ST} events that do not appear to have normal recovery phases. These events have D_{ST} negative intensities that arc relatively constant for days on end, Two good examples of this feature are present on days 52-60 and 135-138. Days 135-138 arc shown in higher temporal resolution in Figure 3. The panels arc: the solar wind plasma parameters plus interplanetary magnetic field components and magnitude, and D_{ST}. There is a small precursor stream on day 134 (Figure 1) prior to the sequence 1 stream. in Figure 3, the slow rise in velocity of the sequence 1 stream starts near the end of day 135 and continues throughout day 138. D_{ST} lies between - -10 nT and -50 nT for these four days.

Thus, this region of more-or-less continuous 10W-ICVCI D_{ST} occurs both on the trailing edge of the precursor stream and on the leading edge of the larger sequence 1 corotating stream.

The average D_{ST} is --25 nT, but shows great variability. Short-term decreases in D_{ST} arc clearly reflected in increases in AE. The one-to-one correspondence between substorms (AE) and ring current increases (D_{ST} decreases) can be interpreted as ring current injection duc to substorm events. The sporadic injections presumably prevent a full recovery of the ring current to quiet-day values. These substorms arc caused by negative B_Z components which are parts of large amplitude Alfvén waves. Such a relationship between southward B_Z, AE increases and D_{ST} decreases can be noted in the Figure.

All of the other long duration recovery phases and small storms without classical recoveries are associated with HILDCAA events. These in turn arc associated with large amplitude Alfvén wave events where the wave components have significant negative B_Z component.s.

Positive D_{ST} Intervals

Two other features in the D_{ST} plot arc noteworthy. One is that there arc several intervals where D_{ST} has positive (~+10 to +20 nT) values for several days at a time. These features can be related to specific solar wind parameters. Examples of positive D_{ST} events are found on days: 14, 40, 50, 78, 105, 132, and 227. The onsets of these events are gradual and the magnitude of D_{ST} typically increases with time. The events start days before the appearance of the high speed streams. Each event is associated with a slow solar wind stream located between the two high velocity coronal hole streams. For the events mentioned above, the minimum solar wind velocity was approximate] y: 350, 310, 330, 330, 310, 330, and 300 km s^{-1}, respectively.

Quiet AE Intervals

Intervals of low geomagnetic activity have been noted as well (see Figure 1). There are small intervals where AE is less than 200 nT for days at a time. These events arc found to be typically associated with intervals that precede the onset of the high speed corotating streams. Examples of events somewhat prior to (but not exactly at) the sequence 1 streams arc found on days 21-24, 49-50, 76-78, 102-106, 130-133, 156-158, and 224-230. Each of these intervals also partially overlaps with intervals where D_{ST} is positive.

Five of the seven low AE events mentioned above had common interplanetary features. In these cases, the velocities decreased from 560to310 km s^{-1}, 520 to 300,460 to 360,530 to 360 and 400 to 360 (with a minimum of 300 km s^{-1}), respectively. The magnetic field magnitudes also decreased from 6 to 3 nT, 7 to 5, 6 to 8, 5 to 4, and 5 to 3 nT during these intervals, respectively. The B_Z component variability during these intervals was generally small. There is a general lack of large amplitude Alfvén waves during such intervals.

There arc several plasma features that arc common for the above five events. The events occur on the trailing portions of high speed streams. The velocities start near 500 km s^{-1} and decrease with time. The temperatures also decrease and the plasma densities increase throughout the events. The densities start at very low values, ~3 cm^{-3} and increase to substantial values as the HCS is approached. For the five cases, N increases from 3 to 65 cm^{-3} (just prior to the stream onset and HCS crossing at the start of day 25), 3 to 12 cm^{-3} (including a broad HCS crossing from days 105-106), 3 to 11 cm^{-3} (just prior to a HCS crossing at the end of day 133), 3 to 5 cm^{-3} (just prior to the HCS crossing on day 159) and 5 to 40 cm^{-3} (just prior to the HCS crossing at the beginning of day 231). The higher ram pressures associated with the enhanced interplanetary densities and the lack of ring current energy injections (due to the lack of the presence of negative B_Z) presumably arc the causes of the positive D_{ST} values.

Corotating Streams and their Relationship to HCS Crossings

Prior to the beginning of the event illustrated (Figure 4), the field had exceptionally low values of ~1nT at 1445- 1700 UT day 24 and had an orientation that is neither in a + or - sector polarity (see Figures 1 and 2). The solar wind has an exceptionally low velocity (300-310 km s^{-1}) as well as a low temperature (-2x 10^4 K). The plasma density was high, -20-30 cm^{-3}. These plasma features give a good indication that the spacecraft (and Earth) was near the HCS. The low magnetic field strengths (and therefore low potential B_Z values) cause very low AE values.

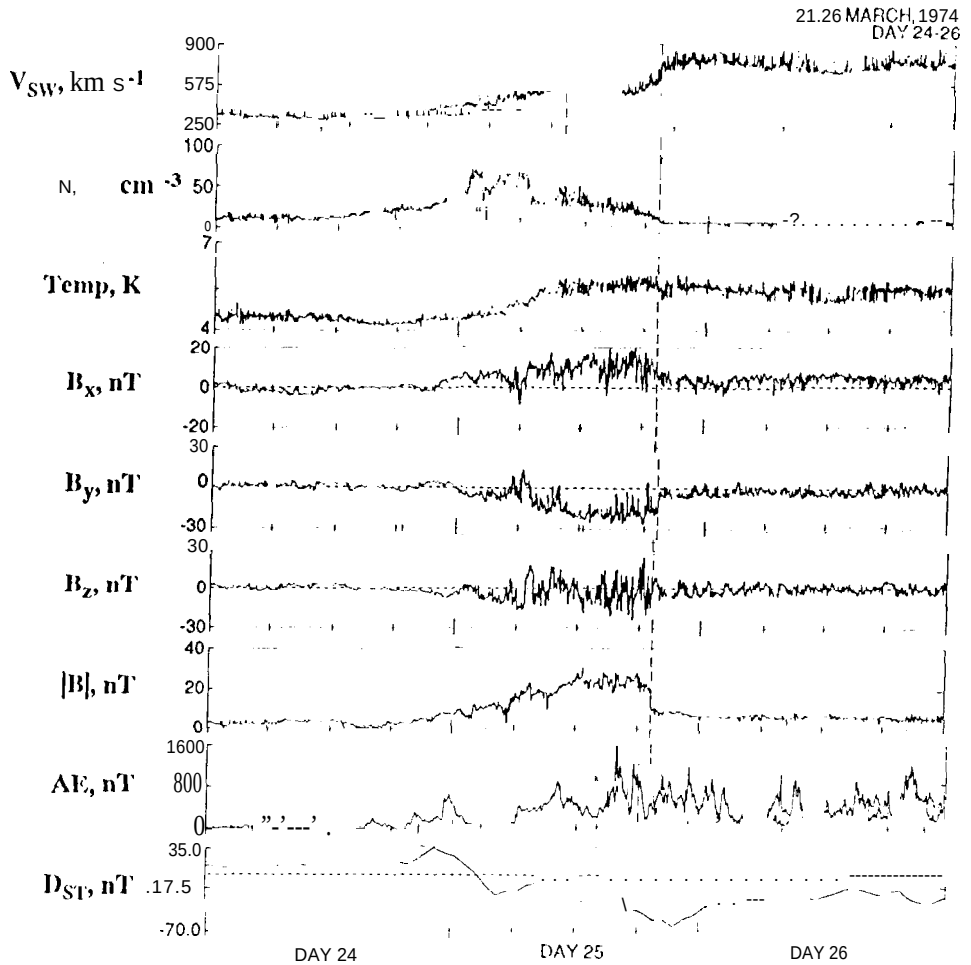

Figure 4. The D_{ST} --65 nT storm created by a corotating stream/heliospheric current shed (HCS) interaction on day 25, 1974!

With increasing time from 1700 UT day 24 to 1200 UT day 25, there are steady trends in several of the plasma parameters. The magnetic field increases from ~1nT to 25 nT. N increases from 15 cm^{-3} to 80 cm^{-3} (at -0500 UT) and then decreases to 30 cm-3. There arc no significant velocity and temperature gradients until -0400 UT day 25. At this time the velocity starts at 330 km s^{-1} and rises, and the temperature starts at 3 x 1 0^4 K and rises . By 1200 UT, day 25, V_{SW} is -450 km S-l and T -5.5 x 10^5 K. The increasing plasma density leads to an increase in the solar wind ram pressure and hence a peak D_{ST} of - + 35 nT at ~02 UT day 25.

Beyond 1200 UT day 25, the velocity continues to increase, reaching a maximum of 775 km s^{-1} at ~0030 UT day 26. The temperature reaches a maximum of ~6 x 10^5 K from 1300 (o 1910 UT day 25 and suddenly decreases to 4 x 10^5 K at 1910 UT. This decrease is due to the presence of a reverse shock. The solar wind velocity jumps from 620 km s-1 to 740 km s1, the density abruptly decreases from 12 to 5 cm^{-3} and the magnetic field magnitude decreases from 22 to 10 nT. This example of a reverse shock occurring at 1 AU without the presence of a forward shock is fairly common in the data studied.

The B_Z that causes the storm is clearly related to the stream interaction with the HCS and its plasma sheet. B_Z steadily decreases from + 3 nT at 1200 UT day 24, to - 10 nT at 0400 UT day 25 as the HCS plasma sheet density increases from 12 to 60 cm^{-3}. The most intense southward B_Z field during the event occurs from 0600 UT to 0655 UT day 25 with a peak intensity of -16 nT. This intense southward IMF is coincident with the magnetic storm onset. The location of this B_Z event is found at the base of the HCS plasma sheet/strcan~ interface. The velocity of the stream is only 370 km s^{-1} at the time. It should be noted that pressure correcti ons have not been removed from D_{ST}. Thus, the D_{ST} values may be significantly lower than indicated, particularly from 12-18 UT day 25.

SUMMARY

Figure 5 illustrates a schematic of the corotating stream interaction with the heliospheric current sheet. At the top of panels 5a) is the quiet solar wind. The view is down from over the north ecliptic pole. At the bottom of the panel, the straight arrows represent the high speed corotating stream. The interaction of this stream with the HCS leads to compression of the field and plasma, enhancing both the plasma densities and the magnetic field magnitudes. Because of the curvature of the magnetic fields, this stream-stream interaction is only a glancing onc and yields only a slight compression.

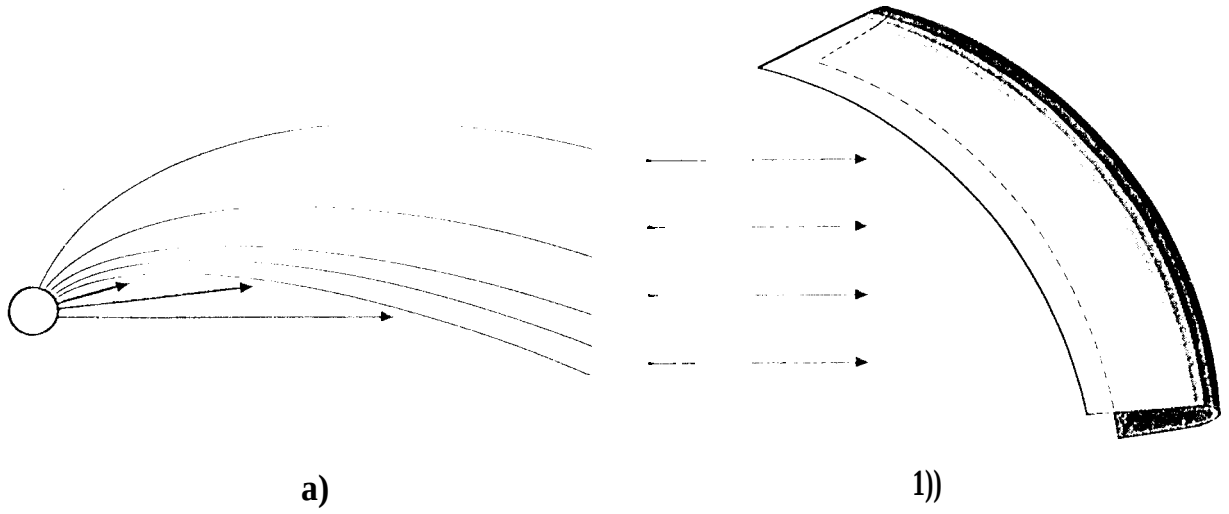

a) 1))

Figure S. Schematics of the corotating stream-l ICS interaction: panel a) view from the north ecliptic pole, and b) view from the ecliptic plane.

The bottom panel, 5b), shows a side view from the ecliptic plane. Here wc have drawn the HCS with a substantial north-south orientation. The fast-stream interaction will distort the shape of the HCS and fields draped around this structure. Random north-south B_Z components will be created from this interaction, leading to small storms.

A schematic of the interplanetary features causing geomagnetically active and geomagnetically quiet intervals is given in Figure 6. Region (1) is the trailing portion of a high speed stream. The velocity is relatively low and it is decreasing with time. The magnetic field magnitude is low and devoid of Alfvén waves. This is a region where AE is lowest (other than times when B_Z is northward for long intervals of time). In region (2), the

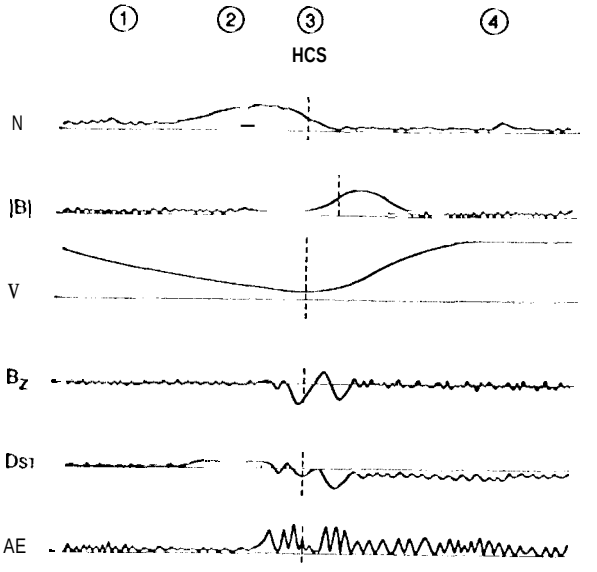

Figure 6. A schematic of the solar wind causes of geomagnetic quiet, HILDCAAs and small magnetic storms during the descending phase of the solar cycle.

plasma density is high duc to the presence of naturally occurring high densities near the HCS and also due to stream-stream compressive effects. This region, when incident on the magnetosphere, leads to positive D_{ST} values through ram compression effects. If the IMF has significant southward components after the passage of this density enhancement, then this positive D_{ST} will appear as an initial phase of the storm (without a sudden commencement). If there are not trailing southwardly directed fields, this will only be a positive D_{ST} event. Region (3) has the high magnetic fields associated with the HCS plasma sheet and the stream-stream compressive effects. Distortions of the HCS and related high fields cause north and south deflections, and the latter leads to weak or moderate magnetic storms. Note that at 1 AU these high field regions are located at the beginning of the gradients of the high speed streams, and arc not near the regions where the gradients or velocities are the highest. Region (4), at the peak and trailing portions of the high speed stream, is characterized by Alfvénic fluctuations in B_Z and concomitant continuous auroral activity (HILDCAAs).

Acknowledgments. Portions of this work were done at the Jet Propulsion Laboratory, California Institute of Technology, Pasadena, under contract with the National Aeronautics and Space Administration.

REFERENCES

Bartels, J., "Some Problems of terrestrial magnetism and electricity" in *Terr. Msg. Electr.*, cd. by J. A. Flemming, McGraw-Hill, 385, 1938.

Chapman, S. and J. Bartels, *Geomagnetism, I*, Chapter XII, 396, Clarendon Press, Oxford, England, 1940.

Farrugia, C. J., L. F. Burlaga, V. A. Osherovich, I. G. Richardson, M. P. Freeman, R. P. Lepping, and A. J. Lazarus, A Study of an expanding interplanetary magnetic cloud and its interaction with the Earth's magnetosphere: The interplanetary aspect, *J. Geophys. Res.*, 98,7671, 1993a.

Farrugia, C. J., M. P. Freeman, L. F. Burlaga, R. P. Lepping and K. Takahashi, The Earth's magnetosphere under continued forcing: Substorm activity during passage for interplanetary magnetic cloud, *J. Geophys. Res.*, 98, 7657, 1993b.

Hundhausen, A. J., Sizes and locations of coronal mass ejections: SMM observations from 1980 and 1984-1989, *J. Geophys. Res.*, 98, 13177, 1993.

Klein, L. W. and L. F. Burlaga, Interplanetary magnetic clouds at 1 AU, *J. Geophys. Res.*, 87, 613, 1982.

Low, B. C. and D. F. Smith, The free energies of partially open coronal magnetic fields, *Ap. J.*, 410,412, 1993.

Smith, E. J. and J. H. Wolfe, Observations of interaction regions and corotating shocks between one and five AU: Pioneers 10 and 11, *Geophys. Res. Lett.*, 3, 137, 1976.

Svalgaard, L., Interplanetary sector structure 1947-1975, Report 648, Inst. Plasma Res., Stanford Univ., Stanford, California, 1976.

Wolfson, R., C. Conover and R. M. E. Illing, The evolution of a coronal streamer prior to mass ejection, *J. Geophys. Res.*, 92, 13641, 1987.

Zirker, J. B., *Coronal Holes and High Speed Wind Streams, CO].* Asso. Univ. Press, Boulder, co., 1977.